RADIATION PROCESSING OF INHOMOGENEOUS OBJECTS AT THE $300\,MeV$ ELECTRON LINEAR ACCELERATOR

O.A. Demeshko, S.S. Kochetov [*]***, L.A. Mahnenko, I.V. Melnitsky, O.A. Shopen***

National Science Center "Kharkov Institute of Physics and Technology", 61108, Kharkov, Ukraine

(Received July 26, 2007)

Comparison is made between the calculated and experimental doses absorbed by complex density-inhomogeneous objects during their radiation processing. The process of fast electron passage through the object and depth dose formation has been simulated by the Monte Carlo technique with the use of the licensed program package PENELOPE. The calculated and experimental data are found to be in good agreement (≈30 %). Preliminary simulation of the process of object irradiation at given conditions provides the necessary information when developing the methods for a particular group of objects. This is of particular importance at performing bilateral irradiation, when an insignificant density variance of different objects may lead to appreciable errors of dose determination in the symmetry plane of the object.

PACS: 87.80.+s, 87.90.+y

1. INTRODUCTION

The expediency of using this or that irradiation technique is determined with consideration for optimum combination of productivity and quality of the given process, which is characterized by the ability to form the radiation field that provides the necessary uniformity of absorbed energy distribution throughout the irradiated object.

The absorbed dose built up on the object surface (in the superfine layer of the material) is determined by the incident electron flux density. In our case, the sweeping magnets are absent, and the output beam has the Gaussian distribution of flux density in the cross section. Therefore, the highest flux density on the object is found on the optical axis of the beam, and its root mean square (r.m.s.) radius is dependent on the initial electron energy, on the material and thickness of the foil of the exit window of the channel, and also on the distance to the object. These initial parameters are chosen in each particular case, depending on the vertical dimensions of the object and the permissible dose variations at the edges (e.g., no more than ≈ 30 %).

2. SHORT DESCRIPTION OF THE FACILITY PARTS AND THEIR FUNCTIONS

The sterilization facility consists of three main parts:

– accelerated electron source with a horizontal beam layout;

– extraction, beam-shaping and beam property diagnostic channel;

– conveyor for object transfer to the irradiation area (see. Fig.1).

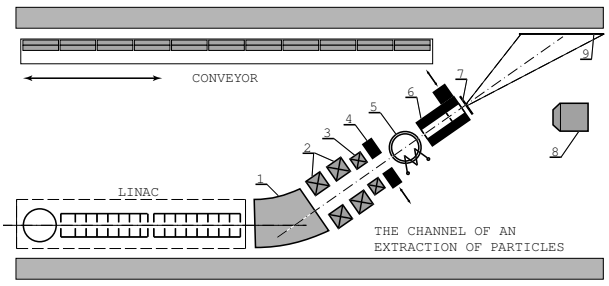

Fig.1. *The lay-out diagram of inventory of the sterilization stand (plan view)*

The accelerated electron accelerator presents a pulsed two-section travelling-wave linear accelerator with adjustable parameters of the beam (mean electron energy 5...25 MeV, half-width ∼ 10 %, average beam current 1...100 μA). It is a complicated setup that incorporates a unique pulse and high-frequency equipment of total power ∼ 90 kw.

The extraction channel includes a dc magnet (1) that deflects the electron beam through 35° in the horizontal plane relative to the accelerator axis. In

[*]Corresponding author. E-mail address: kochetoff@mail.ru

the focus of the magnet there is a particle monochromator (4) intended to analyze beam energy characteristics.

At the channel output, a Faraday cup (6) with a remotely introduced absorber is installed to measure the total beam current. The quadrupole-lens doublet (2) provides beam shaping of r.m.s. radius $0.5\,cm$ at the channel output. A two-pole electromagnetic corrector of horizontal/vertical deflection (3) serves for beam displacement within small limits (approximately $1.5\,cm$) relative to the optical axis of the extraction channel in the conveyor plane. The shape, lateral dimensions and position of the beam during pretuning of the accelerator in the specified operating conditions are controlled with the help of the television facility (8) through the use of the fluorescent screen (7). The refinement of both the beam position and the vertical current density distribution directly on the object at the final adjustment of the operating conditions and further on in the process of the whole irradiation run of the accelerator is realized with the help of the ionization detector (9). In this case, the beam current is continuously controlled by means of an induction transit-time pickup (5), a charge integrator and a digital voltmeter pre-calibrated against the full-absorption Faraday cup (6).

The conveyor presents a horizontal shelf, $25\,cm$ in width and $8.25\,m$ in length. It is assembled from thin plates and duralumin L-shaped elements and is check clamped to four separate carriages movable on rolls along a straight monorail. The asynchronous motor connected with the carriages via a double-reduction worm-gear unit, pinion and chain drives, a lead drum and a haulage line serves as a driving actuator. Irrespective of charging by weight, the conveyor is moving at a constant velocity of $5.1\,cm/s$.

The conveyor performs the number of total cycles or half-cycles (odd number of passes) assigned by the operator through the use of the controlling system in the autoreverse mode at the beginning and the end of one-direction pass, which makes $9.1\,m$ at most. Depending on the conveyor occupancy with objects, the pass length can be regulated. After the assigned program is completed, the beam is switched off and the conveyor stops.

The facility is provided with safety locks for the cases of unforeseen beam switching-off (the conveyor is then stopped) or conveyor stop (in this case the beam is switched off). In case of these unforeseen stoppages, the data are recorded on the number of passes made, the current condition of the conveyor and the direction of its motion at the moment of stoppage. This permits the conveyor restart after troubleshooting with keeping the control over the process of necessary dose buildup by the objects under irradiation.

3. CHARACTERIZATION OF OBJECTS UNDER IRRADIATION

The surgical suture materials (polished catgut, silk suture) are the principal items for treatment. The Customer supplies them for irradiation in the form of ampoules or packets. Separate items are placed in cardboard panels, i.e., boxes, which are then linked in paired units - irradiation objects. The object is characterized by a molecular composition of component mixture, overall dimensions, the average density and density distribution uniformity in the volume. The catgut blocks in ampoules, the lower part of which (without a cardboard box) has an average density of $\sim 1.07\,g/cm^3$ (air, glass, solution, catgut) and the upper part has a density of $\sim 0.43\,g/cm^3$ (air, glass), present more complex objects for irradiation. The irradiation technique under development must take into account these circumstances.

4. DETERMINATION OF AVERAGE DENSITY AND MASS BRAKING POWER OF THE OBJECT

The mass braking power of the object, which involves energy losses dE as a result of collisions and radiation on the path dl (ionization and radiation losses) is the quantitative characteristic of the interaction between the accelerated electrons and the substance of density ρ that is responsible for the absorbed dose. In the case, where the nuclear reactions can be neglected, the total mass braking power of the substance is represented by two components:

$$\varepsilon_{tot} = \frac{1}{\rho}\cdot(\frac{dE}{dl})_{tot} = \frac{1}{\rho}\cdot(\frac{dE}{dl})_{col} + \frac{1}{\rho}\cdot(\frac{dE}{dl})_{rad}\,. \quad (1)$$

There are corresponding detailed tables [1] for the data. However, as mentioned above, the task difficulty in our case lies in the fact that we are dealing with a complex multicomponent composition of the object under irradiation (air, glass, spirit aqueous solution, catgut).

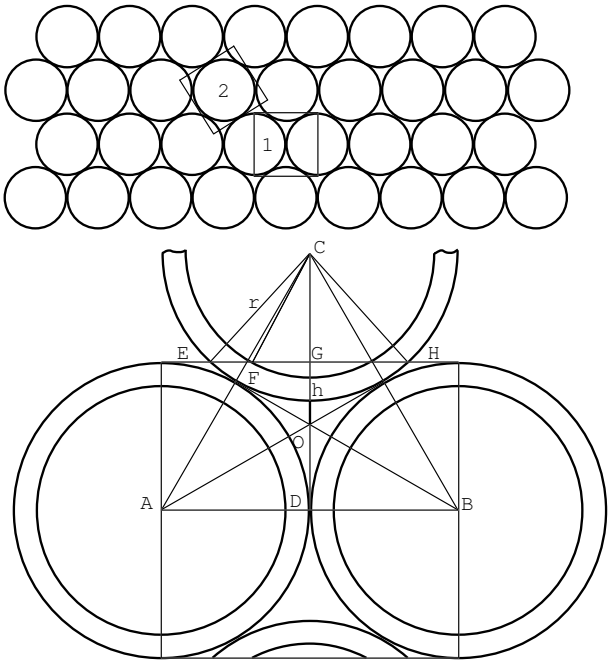

Fig.2. *Element of volume*

Therefore, when estimating the absorbed dose at the given point of the object we must use certain averaged values of energy losses and density.

For averaging of ε_{av} we single out the element of volume in the form of a cube with a side $2r$ (r is the outer radius of the ampoule, see Fig.2). Then, it can be written down the following:

$V_i = S_i \cdot 2r$-partial volume of the i-th component of the object (where S_i- is the cross section);

$m_i = V_i \cdot \rho_i$-partial mass of the i-th component;

$M = \sum V_i \cdot \rho_i$-the total mass of volume element (over all 4 components);

$\rho_{av} = \frac{M}{(2r)^3} = \frac{1}{2r} \sum \Delta l_i \cdot \rho_i$-average volume of the object (were $\Delta l_i = \frac{S_i}{2r}$-is the reduced layer thickness of the i-th component in the volume element)

$\Delta E_i = \varepsilon_i \cdot \rho_i \cdot \Delta l_i$-electron energy losses in the i-th layer;

The average mass braking power of the object takes on the form:

$$\varepsilon_{av} = \frac{1}{\rho_{av}} \cdot \frac{1}{2r} \cdot \sum \varepsilon_i \cdot \rho_i \cdot \Delta l_i \,. \qquad (2)$$

The procedure of determining S_i and Δl_i can be understood from the geometrical constructions presented in Fig.2, which shows the cross section of the volume element (one of possible variants). The calculated ε_{av} values enable one to calculate the surface dose distribution on the objects by the following formula:

$$D \approx \frac{n \cdot I_0 \cdot \varepsilon}{\sqrt{2\pi} \cdot e \cdot \sigma \cdot \nu_n} \cdot \exp(-\frac{y^2}{2\sigma^2}) \,, \qquad (3)$$

were I_0-is the average beam current; e-is the electron charge; σ-is the r.m.s. beam radius; $\nu_n = \nu \cdot \cos\alpha$-is the velocity of the cross motion of the object relative to the beam; n-is the number of conveyor passes; ν-is the linear velocity of conveyor motion; α-is the angle between the beam axis and the normal to the plane of object motion; y-is the vertical coordinate of the reference point of the object.

5. OBJECT SURFACE/DEPTH DISTRIBUTIONS OF THE DOSE

Figure 3,a shows the vertical surface-dose distribution at irradiation of density-uniform object, namely, packeted catgut, 10 cm in height. The r.m.s beam radius on the near plane of the object is $\sim 6\,cm$, the irradiation is bilateral.

A more complicated task relates to the determination of depth dose of the object, particularly if the medium is inhomogeneous. The depth dependence of the absorbed dose is determined by the elemental composition and the average density of the irradiated object, and also by the initial electron energy.

Figure 4,a shows the calculated absorbed dose as a function of depth at energies of 2, 5, 10, 15 and $20\,MeV$ in the elementary case for parallel and uniform-in-the-cross section electron flux incident perpendicularly ($\alpha = 0$) on the semi-infinite medium of density $1.07\,g/cm^3$, which was chosen to be equal to the effective density of the lower part of the object (catgut in ampoules).

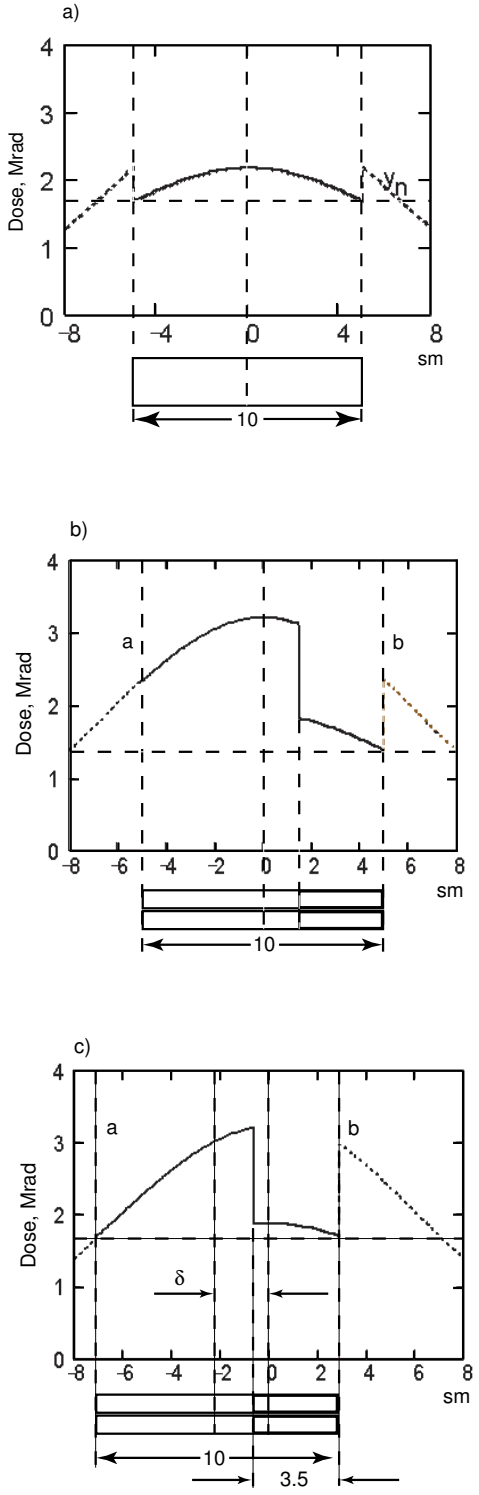

Fig.3. *Height dose distribution at bilateral irradiation of objects: a) density-uniform, b) nonuniform, c) nonuniform with beam displacement by the optimum value relative to the middle of the object*

The process of fast-electron passage through the object and the depth dose formation were simulated by

the Monte Carlo technique with the use of the licensed program package PENELOPE.

PENELOPE provides simulation of arbitrary electron-photon showers in complex material structures (mixtures). In the process, consideration is given to the following types of interaction: elastic and inelastic scattering of electrons and positrons, bremsstrahlung by electrons and positrons, positron annihilation, coherent scattering, Compton scattering of photons, electron-positron pair production.

It can be seen from Fig.4,a that the dose increase in the depth medium due to the production of secondary particles is dependent on energy, the dose becoming lower with energy increase.

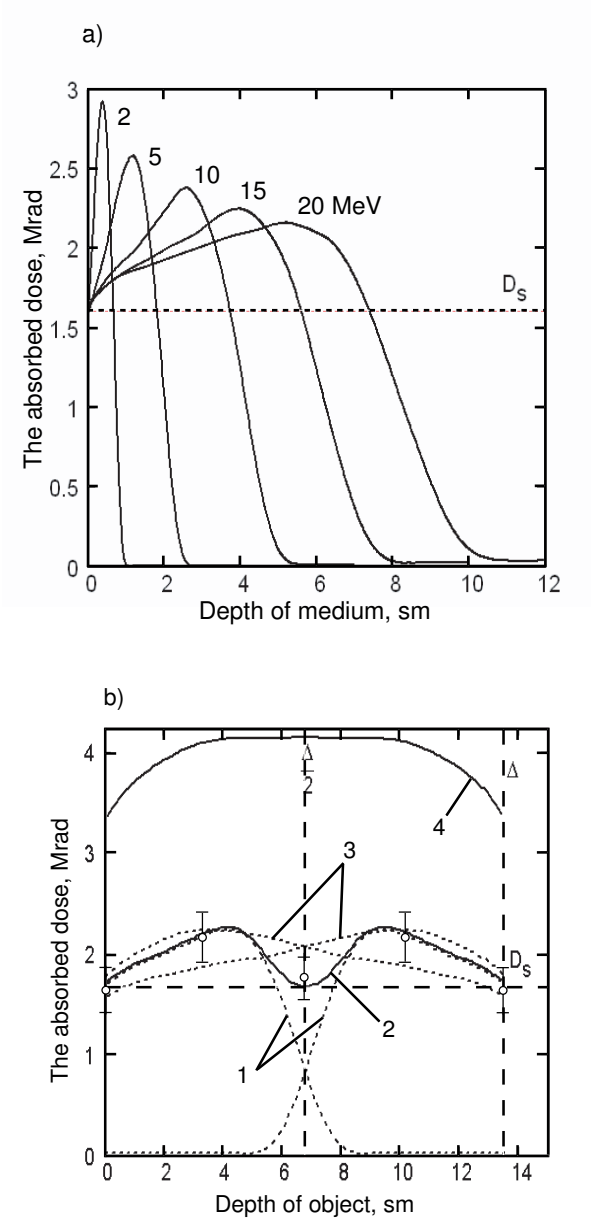

Fig.4. *Depth dose distribution*

To irradiate objects, we have chosen the $(15...16)\,MeV$ energy range, where the dose difference within the object is about $\sim 30\,\%$, and the extrapolated path of electrons in the medium (R) varies between 7.3 and $7.8\,cm$.

To equalize the dose in the depth of the object and to improve the efficiency of the irradiation process, the known bilateral irradiation method is used.

Figure 4b shows the plots of calculated depth dose formation in this case for electron energy of $16\,MeV$ and the above-specified initial conditions (i.e., parallel uniform flux). Calculation was carried out for 6 passes of the standing on the conveyor object, at a current of a beam of electrons $I = 73\,\mu A$. The optimum thickness of the object, at which dose balance is provided both on its surface and inside, is $\Delta \approx 13.5\,cm$. Curves 1 illustrate the data about object irradiation on each side, curve 2 shows the total characteristic.

All other conditions being equal, the dose accumulated in the unit layer of the object is determined by the mass braking power of the object substance and by the density of electron flux passing through it. In our case, the braking powers of materials differ insignificantly. Thus, the decisive role in dose formation belongs to the electron flux passing through the unit layer of the object. At bilateral irradiation conditions, the denser part of the object is irradiated once, while the part of lesser density is irradiated twice in view of its transparence. Hence, at bilateral irradiation the accumulated dose in the part of lesser density of the object is higher than that observed in the denser part.

It is obvious that in the plane of symmetry of the object (this may be the boundary line in the 2-box block) there may be both the lack of dose in relation to the dose accumulated in the thin surface layer Ds, and the excess dose if the real thickness and average density deviate from the optimum values at the set electron energy value.

The same figure also shows the data on the dose field formation in the upper part of the object that has the effective density $\sim 0.43\,g/cm^3$ (curves 3 show the bilateral irradiation data, curve 4 represents the total dose). It can be seen that owing to a relative transparence of the block in this section to accelerated electrons, the absorbed dose substantially exceeds the dose value in the lower, practically nontransparent part that has a higher density (in the figure, the dose curves show only an insignificant step ($\sim 2\,\%$) due to the occurrence of braking gamma-radiation.

Taking into account the facts that the electron flux is divergent, and the current density distribution on the object is nonuniform in the cross section, then, by displacing the optical axis of the beam by a certain δ value vertically downward with respect to the middle of the block, it appears possible to attain the dose equality at the points close to the upper (a) and lower (b) boundaries of the block. (see Figs.3,b,c). This procedure also leads to some increase in the irradiation efficiency and to the decrease in dose straggling directly in the thread field. In this case, the necessary displacement value is determined through

calculations and is adjusted experimentally for each type of objects ($\delta = 1.5...2.5\,cm$).

Since the beam is incident on the object at an angle $\alpha = 55°$, the geometric thickness of the block must be smaller than the above-mentioned Δ value by a factor of $1/\cos\alpha \approx 1.74$. So, at an ampoule outer diameter of $1.1\,cm$, the actual optimum block thickness will be equivalent to approximately 8 layers of closely packed ampoules, i.e., each box must contain 4 layers.

From the above reasoning it is recommended that in the manufacture of the ampoule catgut special care should be taken to control that the spirit solution fully covers the catgut thread in the vertical position of the ampoule. Otherwise, during bilateral irradiation, the part of thread bundle projecting over the solution will receive an excessive dosage by virtue of a considerably lower effective density of the object in this section.

6. CONCLUSION

The computations of the surface absorbed dose by formula (3) and depth dose distribution with the use of the simulation programs PENELOPE are in good agreement between themselves and with the measurement results, the divergence being no more than 30 %. (The absorbed dose was measured by the known technique through the use of Type SO PD(F)-5/150 film dosimeters and Type SF-46 spectrophotometer).

The preliminary simulation of the process of object irradiation at given conditions provides the information required when developing the technique for a specific group of objects. This is of prime importance in the performance of bilateral irradiation, when an insignificant variation in the density of different samples may lead to appreciable errors in dose determination in the symmetry plane of the object (see Fig.4,b).

References

1. Report of the 35-th International Commissions on Radiation Units and Measurements "Radiation dosimetry: electron beams of energies ranging from 1 to $50\,MeV$ (Russian translation). Moscow: "Energoatomizdat". 1988, p.16-22, 28-34.

ОСОБЕННОСТИ РАДИАЦИОННОЙ ОБРАБОТКИ НЕОДНОРОДНЫХ ОБЪЕКТОВ НА 300-МэВ - ЛИНЕЙНОМ УСКОРИТЕЛЕ ЭЛЕКТРОНОВ

О.А. Демешко, С.С. Кочетов, Л.А. Махненко, И.В. Мельницкий, О.А. Шопен

В статье приводятся результаты расчетного и экспериментального определения поглощенной дозы при радиационной обработке сложных неоднородных по плотности объектов. Моделирование процесса прохождения быстрых электронов через объект и формирования глубинной дозы выполнено методом Монте-Карло с использованием пакета лицензионных программ PENELOPE. Расчетные данные находятся в хорошем согласии с экспериментальными ($\approx 30\,\%$). Выполнение предварительного моделирования процесса облучения объектов в заданных условиях дает необходимую информацию при разработке методики для конкретной группы объектов. Это особенно важно при проведении двухстороннего облучения, когда незначительные отклонения плотности разных объектов могут приводить к заметным ошибкам определения дозы в плоскости их симметрии.

ОСОБЛИВОСТІ РАДІАЦІЙНОЇ ОБРОБКИ НЕОДНОРІДНИХ ОБ'ЄКТІВ НА 300-МеВ - ЛІНІЙНОМУ ПРИСКОРЮВАЧІ ЕЛЕКТРОНІВ

О.А. Демешко, С.С. Кочетов, Л.О. Махненко, І.В. Мельницький, О.О. Шопен

В статті наводяться результати обчисленого та експериментального визначення поглинутої дози при радіаційній обробці складних неоднорідних за щільністю об'єктів. Моделювання процесу проходження швидких електронів крізь об'єкт та формування глибинної дози виконано за методом Монте-Карло з використанням пакету ліцензійних програм PENELOPE. Обчислені та експериментальні дані добре співпадають між собою ($\approx 30\,\%$). Виконання попереднього моделювання процесу опромінювання об'єктів у заданих умовах дає необхідну інформацію при розробці методики для певної групи об'єктів. Це особливо важливо при проведенні двухстороннього опромінювання, коли незначні відхилення щільності різних об'єктів можуть призводити до помітних помилок визначення дози в площині їх симетрії.